Biochimica et Biophysica Acta, 1189 (1994) 74–80

BBAMEM 76156

Interaction of papaverine with micelles of surfactants with different charge studied by ^{1}H-NMR

Victor E. Yushmanov [b], Janice R. Perussi [a], Hidetake Imasato [a] and Marcel Tabak [a,*]

[a] *Institute of Physics and Chemistry of São Carlos, University of São Paulo, Cx.P. 369, 13560-970 São Carlos, SP (Brazil) and* [b] *Institute of Chemical Physics, Russian Academy of Sciences, 117977 Moscow (Russia)*

(Received 23 February 1993)
(Revised manuscript received 2 September 1993)

Key words: Papaverine; Vasodilator drug; Micelle; Interaction; Surfactant; NMR

The interaction of the vasodilator drug papaverine (PAV) with micelles of surfactants with different charge of headgroups as well as the properties of PAV in D_2O solution were studied by ^{1}H-NMR. At pD values above 6.4 deprotonated PAV molecules tend to precipitate, the signals of the heterocycle protons of solubilized PAV molecules being shifted to high field. At PAV concentration above 1 mM its protons experience upfield shifts which increase with pD value and are due to the stacking of aromatic rings. Incorporation into micelles caused shifts of all resonances. This effect is due to changes in the local chemical environment of PAV rather than to stacking, and, possibly, involves the deprotonation of the N atom of PAV heterocycle. Line broadening of PAV protons at the molar ratio surfactant/PAV > 16 indicated their restricted mobility. Different complexes were formed due to interaction between the heterocycle of PAV and polar headgroups of cationic cetyltrimethylammonium chloride (CTAC) or anionic sodium dodecylsulfate (SDS). The binding of PAV to zwitterionic *N*-hexadecyl-*N,N*-dimethyl-3-ammonio-1-propanesulfonate (HPS) is similar to that of PAV to CTAC. Association constants were estimated from NMR data as 20, 60 and 350 M^{-1} at $pD = 4.9 \pm 0.1$ for HPS, CTAC and SDS, respectively. Thus, the mode of binding of PAV to HPS is defined by the cationic dimethylammonium headgroup fragment, whereas the negative sulfate fragment attenuates the effective charge of HPS headgroup.

Introduction

Papaverine, 6,7-dimethoxy-1-veratryl-isoquinoline (PAV, Fig. 1), possesses a wide range of biological effects, being commonly known as a cerebral vasodilator and smooth muscle relaxant [1]. It is also used in clinics as a cardiac vasodilator, and its direct action upon coronary blood vessels with a reduction in muscular tonus was associated with the response to stimulation of β-adrenergic receptors [2,3]. It has been classified more recently as a nonspecific vasodilator [4]. Biological effects imply interactions of PAV with cellular components (membranes, biopolymers). In fact, it has been recently reported that PAV affects the hemoglobin oxygen affinity both in isolated protein and intact red blood cells [5,6]. Some of the PAV effects immediately involve cellular membranes. In particular, PAV alters a transmembrane potential and its temperature dependence, compensatory flow and membrane conductivity in epithelial and nerve cells in a pH-dependent manner [7,8]. PAV affects ion transport stimulating Na,K-ATPase of nerve membrane [8], and enhances intracellular Ca^{2+} accumulation in different tissues, thus modifying the pharmacological action of other drugs [9]. By changing ion transport, PAV influences Ca^{2+}-dependent action potentials in myocardium depolarized by potassium [10]. In addition to changes in transmembrane ion transport, PAV inhibits the transport of adenine [11], cyclic AMP [12,13] and insulin [12] across the cellular membranes in different tissues.

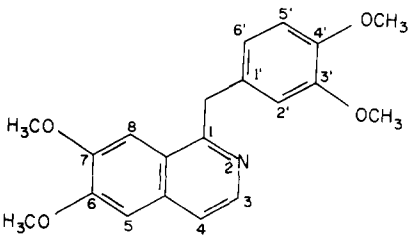

Fig. 1. Chemical structure of papaverine.

* Corresponding author. Fax: +55 162 749163 or +55 162 722218.
Abbreviations: CTAC, cetyltrimethylammonium chloride; HPS, *N*-hexadecyl-*N,N*-dimethyl-3-ammonio-1-propanesulfonate; PAV, papaverine; SDS, sodium dodecyl sulfate.

SSDI 0005-2736(93)E0264-B

Interaction of drugs with membrane lipids defines and modulates other interactions and drug metabolism in organism. However, underlying physico-chemical mechanisms of such interactions quite rarely can be derived immediately from experiments on natural membranes and whole cells. Therefore, various membrane models are in widespread use. Micellar systems, while being the most simple models, provide useful structural and functional models for more complex bioaggregates [14–16]. Understanding of molecular mechanisms of drug–membrane interaction, besides its theoretical importance, has a practical significance for the design of novel drugs and for the selection of the most relevant drugs for various treatment schemes.

This study was initiated in order to gain more insight into both the properties of PAV in aqueous solution and the characteristics of its binding to micellar systems formed by surfactants with different charge of headgroups. Micelles of zwitterionic *N*-hexadecyl-*N,N*-dimethyl-3-ammonio-1-propanesulfonate (HPS) were chosen as a model of lipid aggregates, while cationic cetyltrimethylammonium chloride (CTAC) and anionic sodium dodecyl sulfate (SDS) may be considered as HPS fragments, suitable for studying the interaction of PAV with different parts of the polar HPS headgroup separately. The HPS, CTAC and SDS micelles are commonly accepted model systems for studying various aspects of membrane interactions [17–20]. Proton NMR allowed us to discriminate between different atoms in the PAV molecule during a dynamic equilibrium process in solution. The results could help to elucidate the molecular details of PAV behavior in vivo.

Materials and Methods

Reagents and equipment. PAV hydrochloride (Sigma), HPS (Sigma), SDS (Bio-Rad), sodium acetate (Quimis-Mallinckrodt), D_2O (AnalytiCals), $CDCl_3$ (Aldrich) and Hexane (Chimie-Test) were used as purchased. CTAC (Herga) was purified by acetone-methanol extraction. H_2O whenever used was distilled and deionized. Aqueous solutions were generally prepared in a 0.02 M acetate buffer. The pD values were measured and adjusted using a Corning Model 130 pH-meter by adding 0.4 to the pH-meter readings [21].

Proton NMR spectra were run on a Bruker AC-200 (resonant frequency 200.13 MHz) at ambient probe temperature (23°C). Residual water suppression in proton spectra was achieved using a presaturation by homonuclear gated decoupling during the delay of 2 s between scans. The recycle time was 5.7 s, the band width was 2 kHz, the pulse length was 2 μs. The free induction decay signals were digitized using 16 K data points and processed by an exponential filter with a line broadening factor of 0.2 Hz prior to Fourier transformation.

The IR spectra were measured using KBr pellets on an FTIR spectrometer Bomem MB-102.

Calculations of binding parameters from NMR data. NMR measurements were performed keeping the concentration of PAV constant and varying the concentration of surfactant in the range of 1 to 220 surfactant molecules per PAV molecule. Assuming the complex formation between PAV and surfactant to be a second-order process and that the equilibrium obeys the law of mass action, and taking into account that chemical exchange is fast in the NMR timescale (only single resonance was observed for each PAV proton in all cases), we can write an equation

$$(\delta - \delta_f)/(\delta_b - \delta_f) = K_A S_f/(1 + K_A S_f)$$

where δ, δ_f and δ_b are the observed chemical shifts of a particular PAV resonance and its values for free and bound PAV, respectively; K_A is an association constant for the complex, and S_f is the concentration of the non-bound surfactant. In conditions of a large excess of surfactant $S_f \approx S_0$ (S_0 is the total concentration of the surfactant), and we can determine K_A and δ_b in any linearizing frame (e.g., Scatchard or Hughes-Klotz representations) [22,23].

Results and Discussion

PAV in aqueous solution

The literature data on PAV spectra in aqueous solution are limited and refer to concentrated solution [24]. The spectra of 1 mM and 10 mM PAV solutions in D_2O are shown in Fig. 2A,B. Spectral assignments were made based on δ values and their pD dependences, and confirmed by double resonance experiments. The acidic N^+H proton is not detectable due to the exchange with water. The methylene resonance was observed only if PAV concentration and pD value were relatively high, otherwise it was overlapped by the residual water signal. The same spectra were obtained in H_2O as solvent. The pD dependence of the chemical shift of resonances for PAV in 1 mM solution is presented in Fig. 3. The only appreciable chemical shift alterations at high pD values were observed for the protons of the PAV heterocycle which contains the acidic N^+H group. The pK_a value of this group was estimated as 6.4 by optical spectroscopy (Tabak, M. and Perussi, J.R., unpublished data).

At pD values near the pK_a of PAV, a partial precipitation of PAV occurs. The precipitate was characterized by the disappearance of N^+H resonance and the shifts of other signals in $CDCl_3$ (Fig. 4). IR spectra of precipitated PAV also reveal some peculiarities, the disappearance of an intense line at 2503 cm^{-1} (gener-

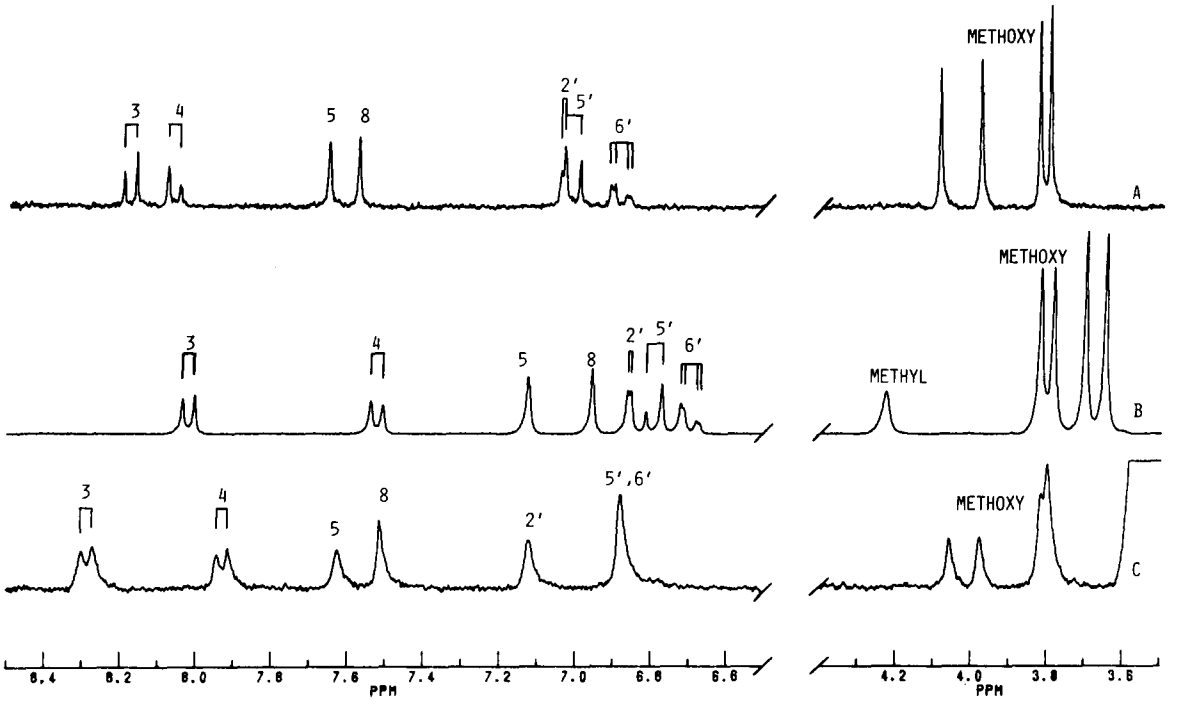

Fig. 2. ^{1}H-NMR spectra of papaverine in D_2O containing 20 mM acetate buffer: (A) 1 mM, pD 4.31; (B) 10 mM, pD 5.60; (C) 0.5 mM in the presence of 64 mM HPS, pD 4.82. The peak numbers for ring protons are given according to Fig. 1. The methylene resonance in charts A and C is overlapped by the residual water signal. The high field part of chart C is distorted by one of the HPS signals.

ally identified as due to amine salts [25]) being the most remarkable. Hence, deprotonated PAV molecules tend to precipitate at high pD values. The data of Fig. 3 at pD = 7.12 are due to the PAV molecules which

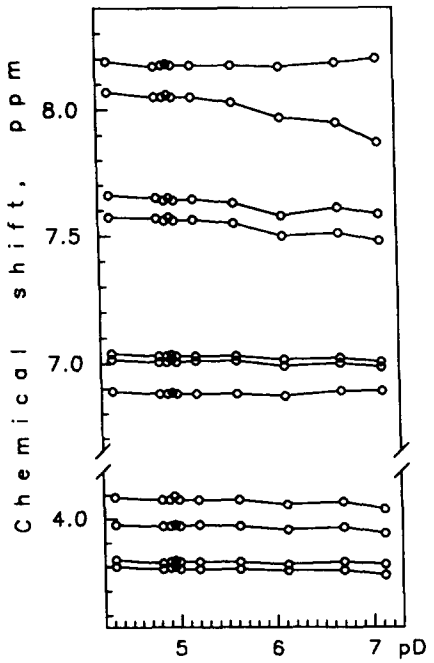

Fig. 3. Proton chemical shifts of 1 mM papaverine in D_2O containing 20 mM acetate buffer at different pD values.

remained solubilized, and can give an idea on the spectrum of the deprotonated PAV in D_2O.

In Fig. 5 the concentration dependence of PAV chemical shifts is presented. At high concentration of PAV in D_2O its protons experience upfield shifts, mainly the protons of the heterocycle. This behavior is known to be characteristic for the stacking of aromatic rings [26,27]. No concentration-dependent changes in peak positions were found using $CDCl_3$ as solvent. Stacking ability of nitrogen heterocycles decreases if nitrogen atom is protonated, i.e., at low pH [27,28]. Accordingly, the higher the pD value, the lower the δ values of PAV protons in 10 mM solution (Fig. 6).

Interaction of PAV with micelles of surfactants

As follows from Fig. 5, the aggregation of PAV was negligible at 1 mM concentration, which still ensured good signal-to-noise ratio in NMR measurements. At concentration above 1 mM stacking introduced a marked effect to the chemical shift measurements. Therefore, the PAV concentration range of 0.5 to 1 mM was chosen for assessing its interaction with micelles.

Incorporation into HPS micelles at pD = 4.9 ± 0.1 caused shifts of all PAV resonances (Figs. 2C and 7). However, the shift patterns were different from those presented in Figs. 3, 5 and 6. Thus, this effect may be ascribed to changes in the local chemical environment

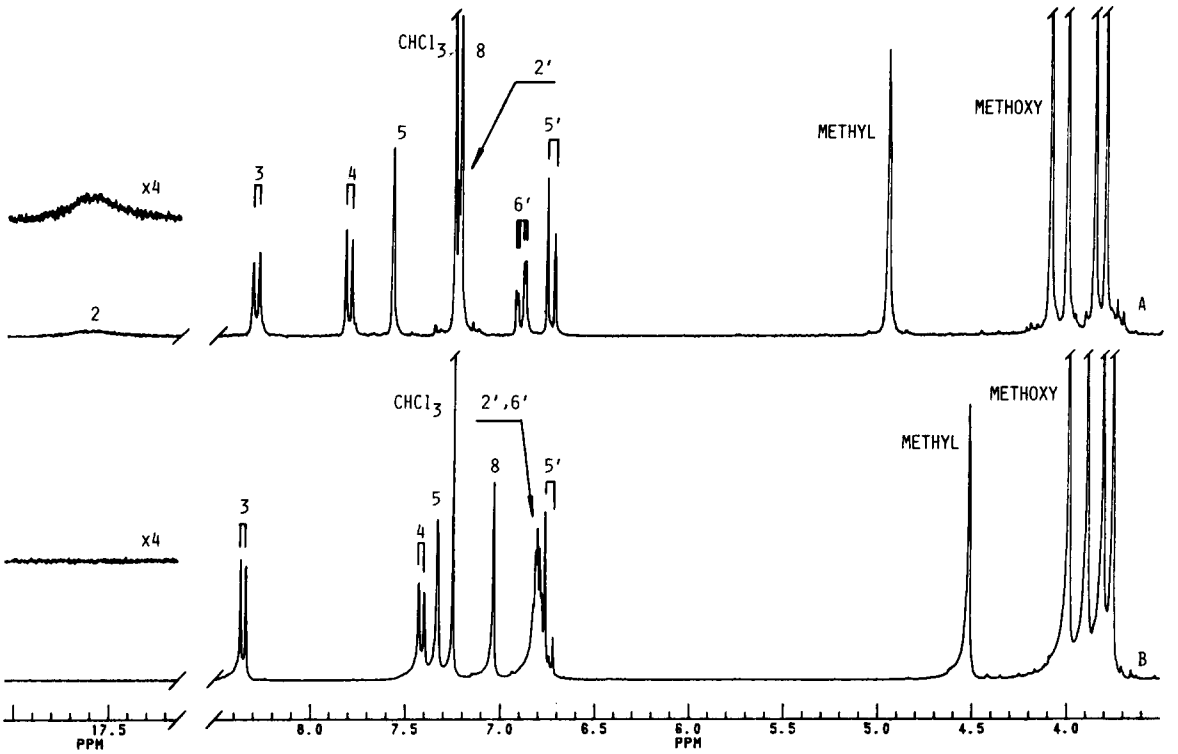

Fig. 4. ^{1}H-NMR spectra of papaverine in $CDCl_3$: (A) hydrochloride; (B) after precipitation from D_2O solution at pD = 12.7. The low field parts in expanded vertical scale are given in the insets.

of PAV rather than to stacking, and, possibly, involves the deprotonation of nitrogen atom of PAV heterocycle.

This result naturally put a question as to which part of the HPS headgroup is responsible for the PAV binding. The sulfate fragment of HPS is closer to the micelle–water interface, therefore, the interaction be-

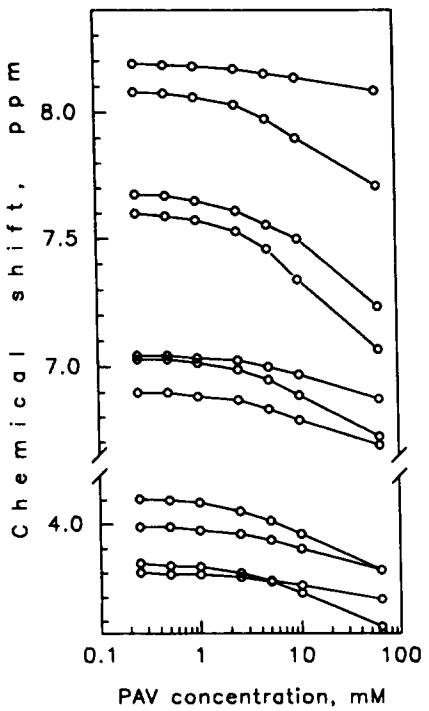

Fig. 5. Proton chemical shifts of papaverine at different concentrations in D_2O containing 20 mM acetate buffer at pD 4.80 to 4.97.

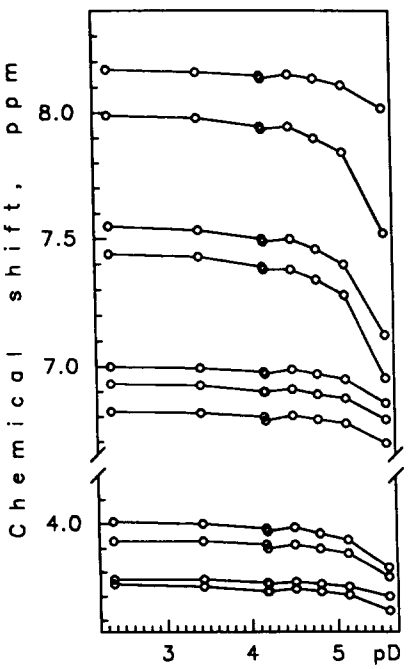

Fig. 6. Proton chemical shifts of 10 mM papaverine in D_2O containing 20 mM acetate buffer at different pD values.

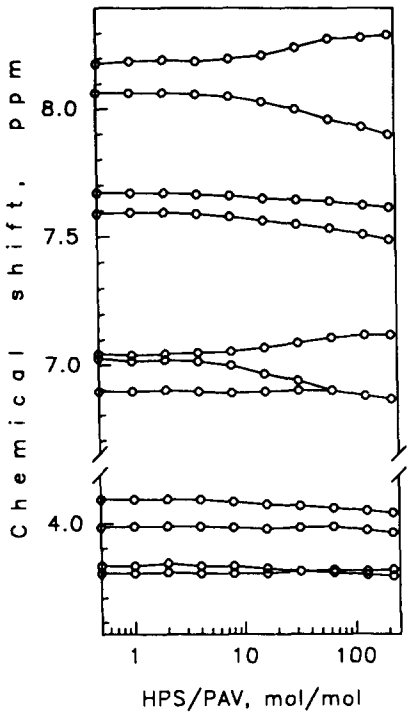

Fig. 7. Proton chemical shifts of 0.5 mM papaverine in D_2O containing 20 mM acetate buffer and variable amount of HPS at pD = 4.9 ± 0.1.

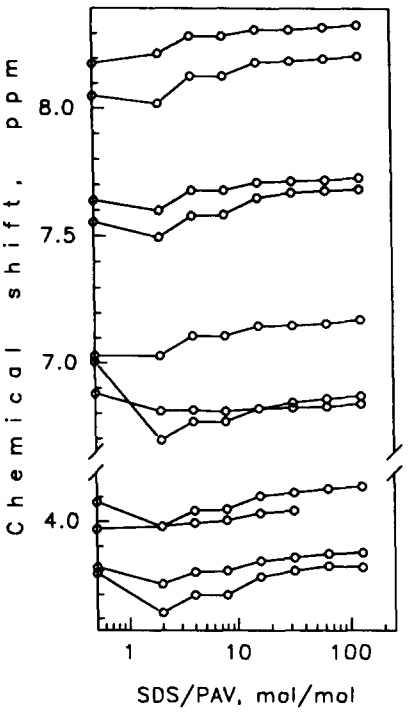

Fig. 8. Proton chemical shifts of 1 mM papaverine in D_2O containing 20 mM acetate buffer and variable amount of SDS at pD = 4.9 ± 0.1. One of methoxy resonances overlapped with the methylene triplet of SDS at 4.04 ppm and was not distinguished at high concentration of SDS.

tween PAV and SDS was studied. At equimolar concentrations PAV and SDS formed a nonsoluble complex. The addition of SDS to SDS/PAV = 2/1 led to resolubilization of PAV in the form of nonmicellar structure, since the concentration of SDS was below its critical micellar concentration. This structure had proton chemical shifts apparently different from those of free PAV in solution (Fig. 8). Following further increase in SDS concentration a new type of complex was formed and dominated at high SDS/PAV ratio (Fig. 8). The chemical shift pattern of this complex has striking differences from that of HPS.

The CTAC titration profiles of chemical shifts of PAV resonances are different from those for SDS titration and qualitatively similar to that for HPS titration (Fig. 9). The interaction of PAV with CTAC and HPS is not merely a hydrophobic interaction with acyl hydrocarbon chains, since PAV is not soluble in saturated hydrocarbons, e.g., hexane.

An appreciable line broadening of PAV signals occurred when the surfactant/PAV molar ratio was equal or exceeded 16 (Fig. 2C). This effect was more pronounced for HPS and CTAC micelles and indicated a restricted mobility of PAV in micelles.

The effects of surfactants on the chemical shifts of PAV protons seemed to be less significant in the case of HPS micelles, other conditions being equal. The obtained data on concentration titration enabled the estimation of both the association constant K_A of the

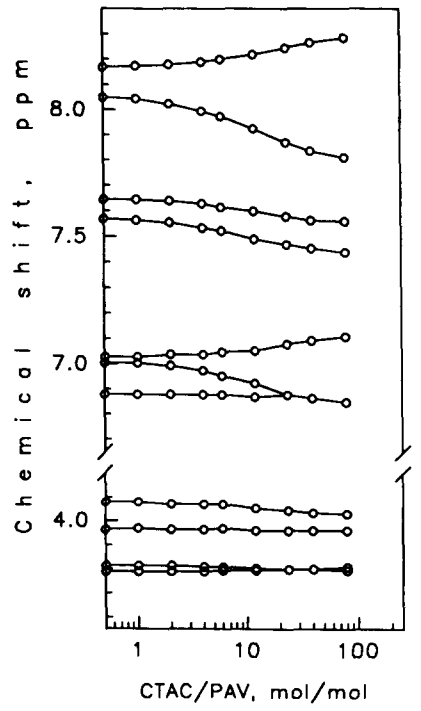

Fig. 9. Proton chemical shifts of 1 mM papaverine in D_2O containing 20 mM acetate buffer and variable amount of CTAC at pD = 4.9 ± 0.1.

TABLE I

Proton chemical shifts (ppm) of papaverine bound to micelles of surfactants in D_2O at pD 4.9 ± 0.1

HPS, *N*-hexadecyl-*N*,*N*-dimethyl-3-ammonio-1-propanesulfonate; CTAC, cetyltrimethylammonium chloride; SDS, sodium dodecylsulfate. See Fig. 1 for numbering of ring protons.

Surfactant	Proton chemical shift (ppm)										
	Ring protons							Methoxy protons			
	3	4	5	8	2′	5′	6′				
HPS	8.35	7.79	7.58	7.43	7.13	6.81	6.81	4.01	3.95	3.81	3.78
CTAC	8.31	7.77	7.54	7.41	7.12	6.82	6.82	4.02	3.96	3.81	3.79
SDS	8.34	8.22	7.73	7.69	7.18	6.88	6.85	4.15	4.06	3.88	3.83

complex and δ_b values for each of the PAV signals. The values of δ_b are indeed characteristic of PAV in the micelle-bound state. Titration curves for different resonances gave approximately the same result for K_A: about 20, 60 and 350 M^{-1} for HPS, CTAC and SDS, respectively, at pD = 4.9 ± 0.1. The values of δ_b given in Table I provide evidence that PAV forms different complexes with SDS and CTAC. The main differences occurred in the δ_b values of the protons of the PAV heterocycle, which apparently interacts in different ways with the cationic and anionic polar headgroups of surfactants. On the contrary, the complexes of PAV with HPS and trimethylammonium fragment of CTAC are similar, indicating that the positively charged dimethylammonium headgroup fragment of HPS defines the mode of binding of PAV to HPS. The sulfate anionic fragment attenuates the effective charge of HPS headgroup, leading to the less significant effects for HPS. It was shown recently that this charge attenuation may result in more weak solvent structure perturbation by HPS as compared with CTAC, due to weaker overall hydration and electrostatic field effects [20]. This was explained by the significant intra- and intermolecular electrostatic interaction between the surfactant head-ions [19].

In conclusion, we have demonstrated that PAV does interact with micelles formed by amphiphilic molecules with different headgroup charge. The aromatic heterocycle of PAV participates in this interaction in different ways dependent on the headgroup charge. The mode of binding of PAV to HPS is defined by the cationic dimethylammonium headgroup fragment, whereas the negative sulfate fragment attenuates the effective charge of HPS headgroup.

Acknowledgements

The authors appreciate the financial support of CNPq and FINEP and a visiting grant to V.E.Y. from FAPESP. The authors are indebted to Dr. P. Berci Jr. for the purification of CTAC and to M.R. Fernandes for FTIR measurements.

References

1 Budavari, S. (ed.) (1989) The Merck Index. An Encyclopedia of Chemicals, Drugs, and Biologicals, 11th Edn., p. 1111, Merck, Rahway, NJ.
2 Pap, J.G. and Fischer, E. (1967) Eur. J. Pharmacol. 2, 1.
3 Charlier, R. (1971) Antianginal Drugs. Handbook of Experimental Pharmacology, Vol. 31, Springer, Berlin.
4 Nikolov, R. and Leniger-Follert, E. (1978) Naunyn-Schmiedeberg's Arch. Pharmacol. 305, 149–154.
5 Meirelles, N.C., Nascimento, O.R. and Tabak, M. (1985) Hemoglobin 9, 399–403.
6 De Paula, E. and Meirelles, N.C. (1992) Braz. J. Med. Biol. Res. 25, 557–565.
7 Simon, L., Porszasz, J., Cibiszerkatalin, P. and Talpas, S.G. (1977) Pharmazie 32, 235–239.
8 Woods, W.T. and Lieberman, E.M. (1976) Neuroscience 1, 383–390.
9 Godfraind, T. (1981) Fed. Proc. 40, 2866–2871.
10 Saguinetti, M.C. and West, T.C. (1981) J. Pharmacol. Exp. Ther. 219, 715–722.
11 Templetom, B.A. and Chilson, O.P. (1981) J. Biol. Chem. 256, 285–290.
12 Campbell, I.L. and Taylor, K.W. (1981) Biochim. Biophys. Acta 677, 357–364.
13 Rindler, M.J., Bachor, M.M., Spitzer, N. and Saier, M.H., Jr. (1978) J. Biol. Chem. 253, 5431–5436.
14 Cordes, E.H. (1973) Reaction Kinetics in Micelles, Plenum Press, New York.
15 Tanford, C. (1973) The Hydrophobic Effect: Formation of Micelles and Biological Membranes, Wiley-Interscience, New York.
16 Mittal, K.L. and Lindman, B. (eds.) (1984) Surfactants in Solution, Plenum Press, New York.
17 Herrmann, K.W. (1966) J. Colloid Interface Sci. 22, 352–359.
18 Reynolds, J.A. (1982) in Lipid-Protein Interactions (Jost, P.C. and Griffith, O.H., eds.), Vol. 2, pp. 193–224, Wiley and Sons, New York.
19 Müller, S.C. and Pottel, R. (1982) in Solution Behavior of Surfactants. Theoretical and Applied Aspects (Mittal, K.L. and Fendler, E.J., eds.), Vol. 1, pp. 485–504, Plenum Press, New York.
20 El Seoud, M.I., Farah, J.P.S. and El Seoud, O.A. (1989) Ber. Bunsenges. Phys. Chem. 93, 180–183.
21 Glasoe, P.K. and Long, F.A. (1960) J. Phys. Chem. 64, 188–190.
22 Wurmser, R. (1973) in Experimental Methods in Biophysical Chemistry (Nicolau, C., ed.), pp. 613–647, Wiley and Sons, London.
23 Dwek, R.A. (1973) Nuclear Magnetic Resonance (NMR) in Biochemistry. Applications to Enzyme Systems, Clarendon, Oxford.
24 Pouchert, C.J. (1983) The Aldrich Library of NMR Spectra, 2nd Edn., Vol. 2, p. 755, Aldrich Chemical, Milwaukee.

25 Silverstein, R.M., Bassler, G.C. and Morrill, T.C. (1991) Spectrometric Identification of Organic Compounds, 5th Edn., p. 160, Wiley and Sons, New York.
26 Cohen, J.S. (1969) Nature 223, 43–46.
27 Granot, J. and Fiat, D. (1977) J. Am. Chem. Soc. 99, 4963–4968.
28 Antonovsky, V.L., Gukovskaya, A.S., Nekrasova, G.V., Sukhorukov, B.I. and Tchervin, I.I. (1973) Biochim. Biophys. Acta 331, 9–20.